# NJC

Accepted Manuscript


This is an *Accepted Manuscript*, which has been through the Royal Society of Chemistry peer review process and has been accepted for publication.

*Accepted Manuscripts* are published online shortly after acceptance, before technical editing, formatting and proof reading. Using this free service, authors can make their results available to the community, in citable form, before we publish the edited article. We will replace this *Accepted Manuscript* with the edited and formatted *Advance Article* as soon as it is available.

You can find more information about *Accepted Manuscripts* in the Information for Authors.

Please note that technical editing may introduce minor changes to the text and/or graphics, which may alter content. The journal's standard Terms & Conditions and the Ethical guidelines still apply. In no event shall the Royal Society of Chemistry be held responsible for any errors or omissions in this *Accepted Manuscript* or any consequences arising from the use of any information it contains.

ROYAL SOCIETY OF CHEMISTRY

www.rsc.org/njc

Journal Name

RSCPublishing

ARTICLE

# Application of an optimized electrochemical sensor in astaxanthin antioxidant properties monitoring against lipoperoxidation, during algae accumulation

Cite this: DOI: 10.1039/x0xx00000x

Received 00th January 2012,
Accepted 00th January 2012

DOI: 10.1039/x0xx00000x

www.rsc.org/

Ramona Penu [*a,b], Simona Carmen Litescu [a†], Sandra A.V. Eremia [a], Ioana Vasilescu [a], Gabriel-Lucian Radu [b], Maria Teresa Giardi [c], Gianni Pezzotti [d], Giuseppina Rea [c]

An optimized electrochemical sensor was developed to assess the antioxidant capacity of carotenoids accumulating during the life cycle of *Haematococcus pluvialis* cell cultures. The sensor was improved with a composite renewable surface made of immobilised phosphatidylcholine (PC) on magnetic nanobeads of iron oxide ($Fe_3O_4$), PC/$Fe_3O_4$, and used to monitor the antioxidant properties of the ketocarotenoid astaxanthin against *in situ* generated phosphatidylcholine lipoperoxides. The surface configuration was able to mimic the natural position and orientation of astaxanthin in the cellular membrane, conferring to the whole experimental set-up good sensitivity for reactive oxygen species (limit of detection for peroxyl radicals $9.1 \times 10^{-10}$ mol $L^{-1}$) with a linear response ranging between $10^{-8}$ and $1.6 \times 10^{-6}$ mol $L^{-1}$. The sensor has proved suitable for both batch and flow measurements. The accuracy of the flow measurements was unaffected by the magnetic field intensity. Electrochemical measurements confirmed that natural astaxanthin is a more effective antioxidant than synthetic astaxanthin, vitamin E and lutein, and that the protective effect of astaxanthin correlates with its concentration inside the cell. The new developed sensor is hence useable for *in line* monitoring of whole cell-based industrial bioprocesses for the production of astaxanthin.

[*a] National Institute of Research and Development for Biological Sciences,Centre of Bioanalisys, Bucharest, 296 Splaiul Independentei, 060031, Bucharest, Romania.

[b] University Politehnica Bucharest, Faculty of Applied Chemistry and Materials Science, 1-7 Gh. Polizu Street, 011061, Bucharest, Romania

[c] Italian National Research Council, Institute of Crystallography Departments of Agrofood and Molecular Design, CNR 00015 Monterotondo Scalo, Rome, Italy

[d] Biosensor SRL, Via Degli Olmetti 44, 00060, Formello, Rome, Italy

[†] Corresponding author: National Institute of Research and Development for Biological Sciences, Centre of Bioanalisys, slitescu@gmail.com, Tel:+40212200900, Fax:+40212207695

Journal Name

RSCPublishing

ARTICLE

## Introduction

Plants and microalgae are a rich source of secondary metabolites having preventive and/or protective functions against human diseases. Among these metabolites, carotenoids (e.g. β-carotene, lutein, astaxanthin, etc.) and Vitamin E class (made of tocopherols and tocotrienols) are of interest for the food and pharmaceutical industries. Both classes of compounds are isoprene-derivatives mostly occurring in the photosynthetic membranes where, among other functions, they are involved in antioxidant defence mechanisms [1-3]. Acting mainly as antioxidants their intake in human diet proved to be effective for the prevention of age-related, degenerative and chronic diseases. This therapeutic potential promoted a dramatic increase in their consumption as dietary supplements, and, as a consequence, prompted the development of analytical systems capable to detect their biological properties along the entire production chain[4]. Astaxanthin is a highly bioactive red coloured ketocarotenoids naturally occurring in a wide variety of living organisms. Although synthetic astaxanthin dominates the world market, currently microalgae cultures are extensively used for the industrial production of biomass as astaxanthin source [5-7]. The unicellular green alga *Haematococcus pluvialis* is a commercial natural source of astaxanthin and it is produced in large industrial scale[8-11]. In specific stressful conditions such as depletion of nutrients or exposure to high light, *H. pluvialis* undergoes a morphological transition from green active cells to red cyst cells in which astaxanthin accumulates in the cyst reaching approximately the 5% of cell dry weight[12,13,14]. Thus, the industrial cultivation of *H. pluvialis* encompasses a first stage aiming at improving biomass productivity (in physiological growth conditions), a second phase aiming at increasing astaxanthin accumulation (in stressful conditions), and a final stage of harvesting[15-17]. An intensely monitoring of these processes could strongly ameliorate industrial production yield.

Generally, the antioxidant activity is the ability of a compound (mixture) to inhibit oxidative degradation (such as lipid peroxidation). Several experimental data support the idea that the antioxidant capacity of carotenoids is related to their structure[18], and in particular to the number of conjugated double bounds[19]. Carotenoids have the capacity to trap both lipid peroxyl radicals and singlet oxygen species[20] (that are not quenched by phenolic - like antioxidants). Moreover carotenoids have the benefit of avoiding potential pro-oxidant behaviour due to the presence of the oxo-groups on the side chain. The ketocarotenoid astaxanthin proved to be effective in scavenging hydroxyl-free radicals, the highest damaging free-radical for human beings[21,22] , but it is not a suitable quencher of peroxyl radicals when compared to phenolic antioxidants.

The radical-scavenging properties of astaxanthin relies on specific molecular structure, made of thirteen conjugated double bonds, two oxo-groups in the 4 and 4' position on the cyclohexene ring, and two hydroxyl groups at the 3 and 3' position, that confer it significantly greater efficiency[23,24,25]. Astaxanthin proved to be a better antioxidant than all other carotenoid antioxidants[26] based on its capability to disperse on the cellular membrane. The cellular membrane dispersion occurs by performing links distributed from inside to outside of the cellular membrane[27]. By this way it is ensured both the astaxanthin ability to scavenge the free radicals from cell membrane, via π electron cloud mobility (from polyene chain, as any regular carotenoid), and the compound capacity to scavenge the free radicals from the inner and outer part of the cellular membrane due to the presence of hydroxyl and keto groups from the two ionone rings[19, 21, 23].

Among the overabundance of methods that can be used for the evaluation of the antioxidant or antiradical capacity of a compound[28] (TEAC - Trolox Equivalent Antioxidant Capacity[29,30], TRAP - Total Radical Trapping Antioxidant Parameter[31], LDL - Low density lipoprotein peroxidation[32], DMPD N,N–dymethyl-phenylendiamine dihydrochloride[33], FRAP - Ferric reducing antioxidant power assay[34], ORAC - Oxygen Radical Absorbance Capacity Assay[35], DPPH-dyphenilpicrylhydrazil free radical[36,37], PCL-photochemiluminescence and β-carotene bleaching[38]), only a few (TEAC, DPPH, PCL) are useful for determining the activity of both hydrophilic and lipophilic species, thus ensuring a broader range of potential applications.

Despite the fact that all carotenoids contain an important number of conjugated double bonds, individual carotenoids differ in their antioxidant potential. There are carotenoids unable to exert measurable antioxidant potential in *in vitro* experiments, due to the fact that the used experimental conditions do not take into consideration the carotenoid orientation on cellular membrane which is the main factor affecting the carotenoids efficacy. Currently, rapid screening models able to provide reliable information based on the proper carotenoid orientation in the membrane are lacking. Some studies prove the ability of carotenoids to protect liposomes (either monolayer or bilayer phospholipid vesicles)[39] from singlet oxygen oxidation, but only few demonstrate how the distribution in membrane affect the carotenoids efficacy as antioxidants[40]. Accurate ascription of the antioxidant capacity of carotenoids should be performed only using analytical protocols able to perform an appropriate discrimination between the mechanisms of antioxidant action while mimicking the *in vivo* carotenoid position and distribution at cell membrane level due to modulator effect of carotenoids for lipid bilayers[41,42]. This is necessary because the variability of carotenoids experimental behaviour is related to the difference between the chain-breaking antioxidant activity and the radical-scavenger activity. The lipid/phospholipid membrane or liposomes models started to be used in assessing the antioxidant efficacy of carotenoids[43-45] but most of the published protocols are time-consuming and request heavy equipment (e.g. high performance liquid chromatography with diode array-mass spectrometry detection[39,44]) slowing down the monitoring and harvesting processes of industrial bioprocess.

Accordingly, the development of a rapid screening instrument taking into account all the above mentioned issues and able to provide reliable information on accumulation levels could be of particular industrial interest especially if could provide information suitable to *in vivo* biological activity. The analytical device should consider the specific distribution (position and orientation) of carotenoids on cellular membrane. Electrochemical devices are useful tools to this purpose as they are able to detect either hydrogen atom transfer (HAT) or electron transfer reaction (ET) of the antioxidants[45].

The aim of the present work is to propose a model able to mimic the carotenoid distribution on cellular membrane applicable in designing a measuring system based on an electrochemical sensor. The sensor should provide rapid and reliable information on the carotenoids efficiency as antioxidants. The developed model was obtained by improving a previously reported electrochemical sensors[46,47] to propose a more useful analytical tool providing responses unaffected by memory effects - since a renewable surface is used - and suitable for industrial *in line* applications in terms of stability, sensitivity and versatility for batch and flow measurements. The measuring principle involves the choice of the appropriate oxidizable substrate, in our current work phosphatidylcholine (PC) that is subjected to oxidation by biologically relevant free radicals, peroxyl radicals $ROO^{\cdot}$ [48]. The process is monitored in the presence and in the absence of the antioxidant. The case study for the present report was astaxanthin. The reasons to use phosphatidylcholine as substrate were its ability to provide the appropriate conditions for membrane model, the PC oxidation mechanism that is following the same oxidative path as low-density lipoproteins (LDL) thus generating lipoperoxides in the presence of peroxyl radicals and the better lot-to-lot reproducibility of PC with respect to LDL. The optimised electrochemical sensor was applied to assess the antioxidant properties of astaxanthin accumulating during different stage of growth of *H. pluvialis*, in order to contribute to a better control of the algal growth and harvesting processes.

## Experimental

### Reagents

The used reagents were purchased from the following sources: phosphatidylcholine from egg yolk (PC), 2,2'-azobis (2-methylpropionamidine) dihydrochloride (AAPH) - 97%, potassium chloride (KCl), hydrogen peroxide ($H_2O_2$), potassium ferrocyanide, potassium bromide FT-IR grade, dimethyl sulfoxide (DMSO), sodium dodecyl sulphate (SDS), potassium phosphates, sodium borate, hexane, acetonitrile, lutein and α-tocopherol were Sigma-Aldrich. Fluorescein was sigma Aldrich. Magnetic $Fe_3O_4$ nanoparticles (nanobeads) were provided by Polytechnica University of Bucharest, synthetic astaxanthin was provided by Sigma Aldrich (Astaxanthin ≥98%, HPLC) and astaxanthin from *H. pluvialis* was provided by Algatechnologies Ltd, Israel.

### Design of the measuring system based on a surface renewable electrochemical sensor

The development of the measuring system was based on a previously reported proof of concept electrochemical sensors, and considering the envisaged application for in line measurements, the following experimental steps were fulfilled:

a. stabilisation of composite-phosphatidylcholine PC bound to $Fe_3O_4$ magnetic nanobeads. The procedure is detailed in Litescu et co-workers [47]. Briefly, 72 mg of PC were suspended in 5 mL KCl 0.1 mol $L^{-1}$ by slight PC sonication for 3 minutes, followed by suspending 24 mg of magnetic nanobeads ($Fe_3O_4$) in the previous suspension and vortexed for 18 hours. After that PC-modified nanobeads ($PC/Fe_3O_4$) were separated using a magnetic separator then repeatedly washed, first time with KCl 0.1 mol $L^{-1}$ and subsequently with water, each supernatant part was removed while $PC/Fe_3O_4$ nanobeads were dried at 60°C for 30 minutes and stored at 4°C. The efficient PC deposition on magnetic nanoparticles and storage stability of $PC/Fe_3O_4$ nanobeads were checked by Fourier Transform InfraRed Spectroscopy (FTIR). The role of $Fe_3O_4$ magnetic nanobeads is to ensure the surface renewability thus avoiding the memory effects.

b. $PC/Fe_3O_4$ composite deposition on the surface of the working electrode of the DRP 220AT DropSens screen printed electrochemical cell (working electrode Au-screen printed, AuSPE) was performed according to the measuring system. For electrochemical batch measurements 50 µL $PC/Fe_3O_4$ suspension were deposed on AuSPE electrode, allowed to dry for 30 minutes and $PC/Fe_3O_4$-AuSPE cells were stored at 4°C, under vacuum. Based on the magnetic properties of the $Fe_3O_4$ nanobeads support which is working as PC carrier (as $PC/Fe_3O_4$ composite) when flow measurements were performed the $PC/Fe_3O_4$ pumped in the system were stopped on the surface of AuSPE working electrode by applying a magnetic field on the Delrin® flow cell.

c. assessment of PC peroxidation degree subsequent radical attack using as measuring system $PC/Fe_3O_4$ and peroxyl radicals thermally generated from azo-initiators.

The currently reported methods to evaluate ROS effects against cellular membrane components have the drawback of problematic direct assay due to extremely short free radicals life-time; therefore it is usually preferred to monitor the molecular product of the oxidative stress reaction[49]. This methodology is based on the correlation between the degree of substrate oxidation with ROS concentration. The design of our measuring system started from this correlation and the peroxidation of the used substrate, $PC/Fe_3O_4$, was initiated using peroxyl radicals obtained at a controlled rate: an aqueous solution of free radical azo-initiator, AAPH was left at controlled temperature for the time necessary to induce the generation at constant rate of peroxyl radicals ($ROO^{\cdot}$). The idea was based on the reported data by Niki et co-workers[50]. The generated ROS, $ROO^{\cdot}$, are further capable to induce lipids/phospholipids peroxidation. The model for electrochemical measurements was initially developed for low-density lipoproteins[46] further applied for immobilised PC[47] but needed optimisation in terms of response range, sensitivity and stability. In our measuring system thermal generated $ROO^{\cdot}$ reacted with an electrochemically inactive substrate (PC deposed on $Fe_3O_4$), generating the corresponding peroxides ($PCOO^{\cdot}/Fe_3O_4$) that proved to be electrochemically active. [46, 47]

d. assessment of analytical performance characteristics for optimised sensor in batch and in flow systems and application on antioxidant efficacy assessment.

### Electrochemical measurements

**Batch measurements.** The electrochemical experiments were performed using an UNISCAN PG 580 potentiostat, the electrochemical cell consisting of a DRP-220AT DropSens modified as follows: gold screen printed working electrode (AuSPE) was modified with composite material by dropping suspensions of $PC/Fe_3O_4$ nanoparticles; the counter electrode was printed gold while the pseudo-reference electrode was screen printed Ag/AgCl; supporting electrolyte KCl 0.1 mol $L^{-1}$.

**Flow measurements**. Electrochemical experiments were carried out in flow system involving a Delrin® flow cell where the analysed sample solution was driven with a peristaltic pump. The substrate was introduced into the cell with a constant flow rate. The value of the applied speed was optimised in order to reach the compromise between the best signal to noise ratio while avoiding the surface damage of the composite $PC/Fe_3O_4$; subsequently the corresponding

current-time curves were recorded. Carrier buffer was KCl 0.1 mol $L^{-1}$.

The used techniques were *i)* cyclic voltammetry (CV), on a potential range 1.2 to – 0.4 V *vs.* reference electrode, to perform the system characterisation and to verify the optimum operational parameters for *ii)* chronoamperometric (CA) measurements. The CA measurements were performed applying the optimized reduction potential according to the monitored oxidation product, namely +0.385 V *vs.* Ag/AgCl pseudo-reference electrode. In order to avoid potential electrochemical interferences from gold oxides, prior to AuSPE use, the DRP-220AT cells were slightly sonicated in ethanol for 30 seconds, washed with bi-distilled water, dried and stored under vacuum. A DRP-220 AT cell was used for 35 consecutive flow measurements due to the benefit of using PC/$Fe_3O_4$ renewable surface; when batch measurements were performed the DRP-220 AT cell is of single use. Another operational parameter specific for electrochemical measurements that was optimized was the reaction time between reactive oxygen species and PC/$Fe_3O_4$ to ensure a constant production of phosphatidylcholine peroxides for batch and flow measurements.

**FTIR measurements**

FTIR spectra were recorded at room temperature using a Bruker Tensor 27 spectrometer in angular reflectance and transmittance modes; when necessary inert atmosphere was used in samples compartment. The spectra were collected and ascribed using Opus software. When transmittance measurements were performed the spectral range was 4000 – 400 $cm^{-1}$, the aperture 4 mm, the spectra resolution 4 $cm^{-1}$ and 128 scans were acquired for each spectrum, at 20 Hz. Samples were pressed into a KBr pellet, the background spectrum being recorded against KBr pellet.

**Scanning electron microscopy (SEM) measurements**

The SEM measurements were performed on PC/$Fe_3O_4$ nanocomposite using a FEI Electron Scanning Microscope. The composite nanobeads were deposed on double conductive C ribbon and the SEM images and EDX spectra were acquired at a voltage of 20 kV.

**Astaxanthin extraction from *Haematococcus pluvialis* cell cultures and UV-Vis quantification**

500 mg of dried *H. pluvialis* cells were taken in 3 mL DMSO and mixed with 40 mg of glass beads. The mixture was sonicated for 12 minutes; centrifuged at 4000 rpm for 5 minutes, the supernatant was collected, and, eventually filtered on PTFE filter (4.5 µmesh) (if centrifugation is efficient, filtration is not needed). The amount of dissolved astaxanthin in the collected supernatant was easily estimated by UV-Vis spectrophotometry. A stock solution of 100 µg $mL^{-1}$ astaxanthin was prepared in DMSO and a calibration graph for astaxanthin was drawn (A=f (c)) for the following concentrations of astaxanthin: 0.4 µg $mL^{-1}$; 0.8 µg $mL^{-1}$; 1.6 µg $mL^{-1}$; 3 µg $mL^{-1}$; 5 µg $mL^{-1}$, using as blank DMSO; measurements were performed in UV-Vis cells with 1 cm path, at 488 nm.
Then 50 mL from the supernatant were taken and diluted at 3 mL with DMSO, the absorbency at 488 nm was measured and the obtained value was interpolated on calibration graph to determine the astaxanthin concentration.

**Oxygen Radical Absorbance Capacity measurements**
Experiments were performed using an OCEAN Optics QE Pro-FL fluorescence spectrometer, the diameter of optical fiber being 560 µm. The ORAC assay is based on *in situ* production of peroxyl free radicals generated via an azo-compound, 2,2,-azobis(2-methylpropionamidine) dihydrochloride (AAPH). The peroxyl radical is able to react with the fluorescent probe increasing the rate of fluorescence decay. The fluorescent probe used was fluorescein (FL), excitation wavelength 490 nm, emission wavelength 515 nm. Measurements were performed in phosphate buffer 75 $\times 10^{-3}$ mol $L^{-1}$, pH=7.40 at a total volume of 1 mL, using microemulsions prepared by mixing hexane (0.66% w/w), SDS (4.87% w/w), 2 propanol (6.55% w/w), and $75\times10^{-3}$ mol·$L^{-1}$ phosphate buffer (87.93% w/w) to disperse the investigated lipo-soluble compounds. The micellar environment does not affect significantly the fluorescent emission and the results obtained for Trolox are similar with those obtained in aqueous media. A blank (FL + AAPH) using micellar environment was obtained. Sample curves (fluorescence versus time) were normalized to the blank curve. The results were obtained by calculating the area under the fluorescence curve, and it were expressed as equivalent of micromoles of Trolox per mg standard compound.

## Results and discussion

**Characterisation of designed measuring model based on a surface renewable electrochemical sensor**

**Stabilisation of PC on magnetic nanobeads.** The rationale of developing a new model applicable in the assessment of the antioxidant properties of carotenoids was detailed in the introduction. The basis of our current work is the necessity to ensure an experimental environment able to mimic as closer as possible the position and orientation of carotenoids in the phospholipidic bi-layer of cellular membrane, in order to provide reliable physiological information. By exploiting previously reported data on carotenoids in membrane models and liposomes[41-45] and our group experience in developing electrochemical sensors for ROS and antioxidants monitoring[47], we succeeded to design the model using nanobeads composite PC/$Fe_3O_4$ as renewable oxidizable surface on a conductive solid support (AuSPE).

The preservation of the structural integrity of the immobilized oxidizable substrate was the first critical point addressed in developing our model. This was necessary to provide an instrument able to supply significant data from a physiological point of view on lipoperoxidation. Consequently, subsequent PC immobilization it is compulsory to preserve the main functional groups of free PC availability for radical attack. Structural characterization using FTIR spectrometry was performed for PC-magnetic nanobeads; the spectra were registered for PC free and PC/$Fe_3O_4$ nanobeads composite.

In the case of phosphatidylcholine, the main FTIR absorption bands are, beside the specific bands for methyl and methylene groups in the region 2800 – 3000 $cm^{-1}$, even the band from 1737.4 $cm^{-1}$ ascribable to νC=O stretching vibration for ester group of lipids 1466 $cm^{-1}$ corresponding to $\delta CH_2$ – deformation vibration for methylene group, 1170-1245 $cm^{-1}$ ascribed to $\nu_s$ $PO_2$- asymmetric stretching vibration for phosphate groups and 1063 – 1088 $cm^{-1}$ ascribed to $\nu_s$ $PO_2$- – symmetric stretching vibration for phosphate groups (Fig. 1). The OH groups, either free or involved in intermolecular bounds are present as proved by their specific absorption bands in the 3280 – 3300 $cm^{-1}$ domain. By comparing spectra 1 and 2 it could be concluded that the structural integrity of PC substrate is preserved following deposition, as revealed by the



 

shape and intensity of the specific IR absorption bands. It should be mentioned that the PC quantity was preserved in both measurements in order to properly assign the significant changes in absorption bands intensity. The stability of obtained composite nanobeads, PC/$Fe_3O_4$, was checked in various storage conditions (room temperature and 40° C) for both dried powder and suspension, the powder proving stable for 45 days while suspension loosing stability after 21 days (see supplementary information, Fig. 1S).

It was concluded that subsequent application of the established procedure for PC immobilization on magnetic nanobeads, the recommended storage conditions for composite PC/$Fe_3O_4$ nanobeads are: dried powder, room temperature, no light contact, ensuring by this way a fair stability with respect to envisaged applications of realised composite, namely renewable substrate to study antioxidant preservation against lipoperoxidation. The composite PC/$Fe_3O_4$ so obtained were after that used to test their applicability to monitor the PC peroxidation subsequent to Radical Oxygen Species (ROS) attack.

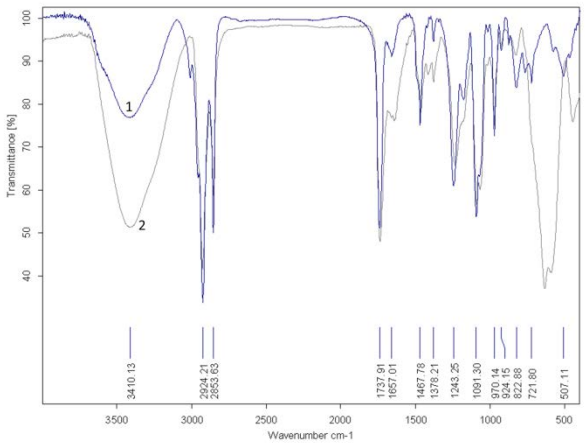


Figure 1. FTIR spectra of nanobeads; PC (1); PC-nanobeads (2)

SEM analysis confirmed the PC/$Fe_3O_4$ nanobeads formation and the complete covering of magnetic nanobeads by phospholipid (Fig. 2) and the preservation of nano-sizes even subsequent PC immobilisation, despite the fact that SEM was not performed in dispersed material but as deposed material. EDX is confirming the PC immobilisation on $Fe_3O_4$ nanobeads by the presence of P, N and C.

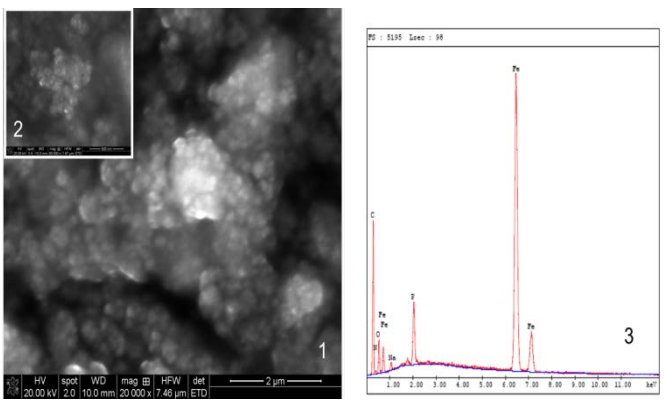


Figure 2. SEM images (1, 2) and EDX spectra of PC/$Fe_3O_4$ nanobeads.

**Assessment of immobilized PC Peroxidation Subsequent ROS Attack .** When cyclic voltammetry experiments are performed with free PC in solution no electroactive characteristics were exhibited, therefore demonstrating that the initial hypothesis was correct, meaning that PC shows a similar behaviour to LDL, with no electroactive characteristics in solution or deposed[47], while in the presence of AAPH generated peroxidation a reduction peak raises (see Fig.3).

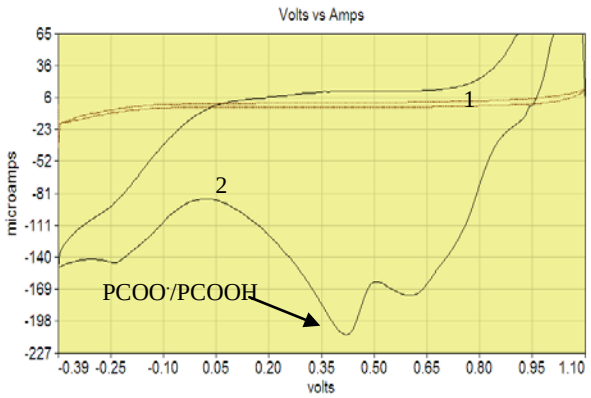


Figure 3. Cyclic voltammograms of PC un-oxidized (1) oxidized (2); (v = 100 mV $s^{-1}$, WE: SPE – Au; KCl 0.1 mol $L^{-1}$)

Subsequent to ROO· generation by thermic reaction, the phosphatidylcholine layer from composite PC/$Fe_3O_4$ was subjected to ROS attack, four redox processes occurring, defined by the following peak potentials: lipoperoxides reduction, $E_{PCOO^{\cdot}/PCOOH}$ = +0.385 (± 0.02) V, and $E_{PCOOH/PC}$ = -0.25 (± 0.02) V respectively; hydrogen peroxide reduction $E_{H2O2/H2O}$= +0.630 (± 0.035) V, the last one involving superoxide evolution on anodic process at +0.920 (± 0.035) V (see figure 2, curve 2).

Considering as significant for lipoperoxides reduction the peak potential $E_{PCOO^{\cdot}/PCOOH}$ = +0.385 (± 0.02) V all further chronoamperometric experiments were performed at this specific value.

**Assessment of PC/$Fe_3O_4$ renewable sensor performance characteristics against ROS attack.** The optimized sensor was characterized considering the sensitive response to free radical attack. In batch system the response of the developed sensor - PC/$Fe_3O_4$ dropped on AuSPE- and ROS concentration were obtained using chronoamperometry. The applied potential value on the working electrode was that defining the reduction of PCOO· species, + 0.385 V *vs.* reference electrode. The variation of the current intensity corresponding to lipoperoxides peak reduction with the concentration of peroxyl radicals was measured. The dynamic range of response was $10^{-8}$ - 1.6 × $10^{-6}$ mol $L^{-1}$, the linear dependence on the concentration range being characterized by the following equation I(nA) = 9.24 × C(nmol $L^{-1}$) - 0.323 ($R^2$ = 0.9913) where C is the concentration of generated free radical species calculated considering the Niki constant rate of radical production[50]. It is known[48] that at 37°C under air, a concentration of 10 × $10^{-3}$ mol $L^{-1}$ AAPH is producing 1.36 × $10^{-3}$ mol $L^{-1}$ $s^{-1}$ free radicals, ROO·; 1 mole of AAPH is producing 2 moles of ROO·[47]. By this way it can be calculated the concentration of ROO· existing in the system per unit of time. In the measuring conditions the obtained detection limit calculated as 3 × S/N was 9.1 × $10^{-10}$ mol $L^{-1}$ for ROO·; the limit of detection was calculated considering the level of noise registered at + 0.385 V in the presence of carrier buffer. The obtained responses (that were the average of 3 measurements) proved that the designed

system is highly sensitive to the extent of peroxyl radicals attack exerted toward the PC layer from composite.

In the same time, to be useful in assessing the antioxidant capabilities, the sensor based on PC/$Fe_3O_4$ composite should respond specifically to the amount of the PC generating $PCOO^{\cdot}$ radicals. Therefore experiments were performed using bare AuSPE electrodes, both in free PC suspensions and in PC/$Fe_3O_4$ suspensions that were immobilised on AuSPE via magnetic field. The response of the sensor was highly influenced by the substrate amount, as noticeable from Fig. 3. The composite modified electrodes act as an insulator when high amounts of PC were used.

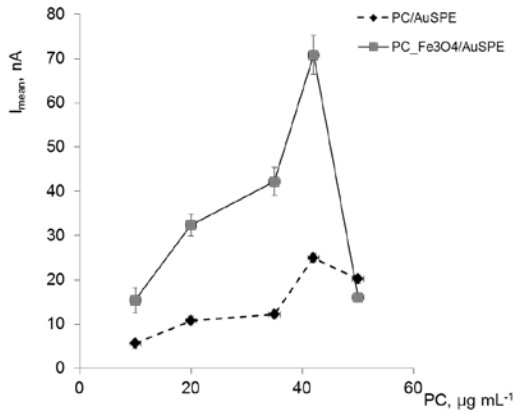


Figure 4. The influence of oxidative substrate concentration on registered signal

When PC/$Fe_3O_4$ nanobeads are stored as powder, as mentioned before, there are stable for 45 days, and the registered response to lipoperoxidation is stable too. After 60 days the intensity of measured current decrease to 91% (± 1.5%) while after 75 days the significant loss on PC intensity bands noticed on FTIR spectra (see supplementary information Fig 1S) is accompanied by a loss of the measured signal, the current intensity decreased to 35% (± 1.8 %). It could be concluded that the lifetime of the sensor is at least 50 days.

**Design of the measuring flow system.** The developed system was designed to be applied for in line monitoring of antioxidants properties; therefore the response of the sensor in flow regime was further tested. Different flow systems configurations were employed for testing the influence of the magnetic field on the registered response and the flow rate influence on the background (noise associated to measurement). The initial flow measures, to test the new designed Delrin cell capabilities of working under a magnetic field, were performed using CA and measuring the potassium ferricyanide reduction on AuSPE in the presence of $Fe_3O_4$ magnetic nanoparticles. Ferro-ferricyanide couple was used as redox probe to test the influence of the magnetic field on the electrochemical response. The switch on/off of the magnetic field faintly influence the measure (the associated noise value was less than 0.15 nA for a response around 1.8 nA), similarly, the flow rate didn't affect the measurement (the flow rate was ranging between 6 and 250 µL min$^{-1}$), see supplementary information, Fig. 2S.

The PC/$Fe_3O_4$ sensor response with variation of peroxyl free radicals concentration was tested in flow, by chronoamperometry. The applied potential was the same potential as in batch, +0.385 V *vs.* screen printed reference Ag/AgCl, and the obtained results proved an operational stability of 5 subsequent measurements (see supplementary information Fig. 3S) the linearity of the response being preserved for AAPH generated peroxyl radicals in the same range as defined for batch measurements.

**Evaluation of magnetic field effect on the registered chronoamperometric response.** Determinations were performed using as significant response of the composite PC/$Fe_3O_4$ nanobeads on peroxidation, in the presence or absence of magnetic field. The used peroxyl concentrations were in the low concentration range 1.6 – 3.5 nmol L$^{-1}$, and the experiments led to the results presented in the table 1.

**Table 1.** Magnetic field influence on chronoamperometric signal (measured as corresponding to $PCOO^{\cdot}$ reduction)

| Peroxyl radical concentration [$ROO^{\cdot}$] nmolL$^{-1}$ | $I_{mean}$ (± SD) nA | |
|---|---|---|
| | No magnetic field | Magnetic field |
| 1.63 | 3.72 ± 0.28 | 4.33 ± 0.09 |
| 2.5 | 8.76 ± 0.49 | 9.60 ± 0.59 |
| 3.82 | 14.03 ± 1.97 | 15.27 ± 0.85 |

n=5 measurements

As could be noticed, the magnetic field has not influenced the accuracy of the sensor response on peroxidation, and consequently, no significant influence is expected when the astaxanthin antioxidant capacity has to be determined. These data confirm the previously performed experiments using the ferro-ferricyanide redox probe.

**The influence of phosphatidylcholine peroxides generation time.** As demonstrated by Niki, the constant rate production of peroxyl radicals depends on the concentration of the azo-initiator in initial solution, the temperature and the time of thermal initiation of free radicals formation. Measurements were performed on the current intensity value corresponding to the reduction of generated PCOOH (PC hydroxy-peroxides) to establish the optimal incubation time between $ROO^{\cdot}$ and PC substrate. The CA measurements in flow were carried out using a PC/$Fe_3O_4$ composite amount able to provide the equivalent concentration of 40 µg mL$^{-1}$ PC, while AAPH initial concentration was 30 × 10$^{-3}$ mol L$^{-1}$. The results, as mean triplicate measurements for entire time range, using 5 injections per each point in two subsequent days of measurements, in similar conditions, are given in Fig. 5.

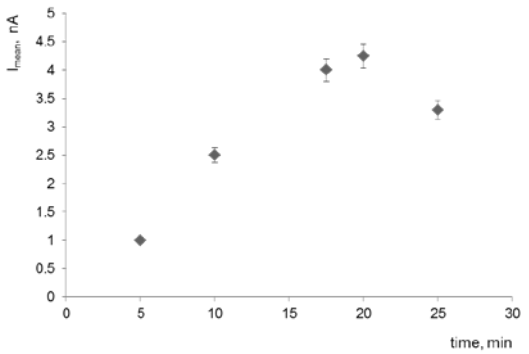


Figure 5. Variation of registered current intensity of $PCOO^{\cdot}$/PCOOH reduction peak with free radical-substrate incubation time

It could be observed that 20 minutes of incubation between PC ($PC/Fe_3O_4$ nanocomposite suspension, equivalent to 40 µg $mL^{-1}$ PC concentration) and AAPH ($30 \times 10^{-3}$ mol $L^{-1}$) at 60° C represents the optimal time to be used for hydroxy-peroxides formation at constant rate. The maximum measured value of the current intensity of $PCOO^{\cdot}/PCOOH$ reduction peak was attained in these experimental conditions.

**The influence of flow rate on the chronoamperometric response.** When a flow measurement is performed, it has to be taken into account the fact that the flow rate is significantly influencing the method sensitivity. Accordingly, the variation of the registered current intensity with the flow rate variation was studied in the experimental conditions mentioned above. The recommended flow rate value was 2.5 mL $min^{-1}$ (Fig. 6) that is quite a high value. This flow rate value is, in fact, correlated to the mechanism of the monitored reaction, which is the fast one being a chain radical mechanism.

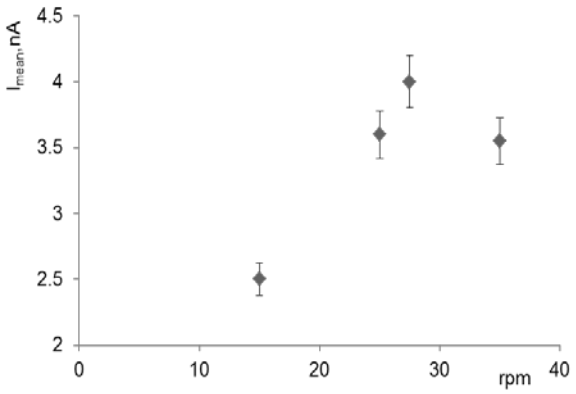


Figure 6. Variation of measured PCOOH current intensity with carrier buffer flow rate

**Application of $PC/Fe_3O_4$ developed sensor in the assessment of lipophilic antioxidants efficacy against PC peroxidation (batch and flow measurements).**

The optimized system was further applied to assess the efficacy of several antioxidants against lipoperoxidation. The developed model was tested for astaxanthin and lutein, to check their antioxidant behaviour against PC peroxidation, since the envisaged applicability of the system is the development of a measuring model able to mimic the membrane distribution of different carotenoid classes. The electrochemical response was tested also for another lipo-soluble antioxidant, namely $\alpha$-tocopherol considering that the reaction antioxidant-quenched free radical is a specific one.

Using the previously optimised incubation time, 20 minutes, the $PC/Fe_3O_4$ on the surface of AuSPE in stopped flow was left to react with peroxyl radicals, $ROO^{\cdot}$, the *in situ* concentration being $1.63 \times 10^{-3}$ mol $L^{-1}$, registered value of current intensity $i_{FR}^{PCOO\bullet}$ being measured on the detector level, corresponding to the PC peroxides formation. On the second detector, simultaneously, the same reaction was allowed to complete together with the antioxidant, in order to estimate in the same conditions the preservative effect of tested lipophilic antioxidants, in this case being measured the current intensity of the reduction peak corresponding to residual PC peroxides $i_{FR+Aox}^{PCOO\bullet}$. Residual PC peroxides are those peroxides un-quenched by the tested antioxidant. The efficacy of the antioxidants preservation was expressed as relative percent of lipoperoxides formation[45]. In this respect it should be mentioned that higher is the percent of measured $PCOO^{\cdot}/PCOOH$ (meaning higher is the value of CA measured current intensity), lower is the antioxidant efficacy.

The efficacy of tested antioxidants was expressed as the relative percent of lipoperoxides formation using the formula:

$$\%PCOO\bullet = \frac{i_{FR}^{PCOO\bullet}}{i_{FR+Aox}^{PCOO\bullet}} \bullet 100$$

The results obtained for batch analysis using standard compounds are given in Fig.7. The first tested astaxanthin was synthetic one. It is noticeable that for membrane model the astaxanthin efficacy is higher than the vitamin E efficacy, the percent of generated PC peroxides being higher when the membrane preservation was ensured by vitamin E with respect to the value obtained for astaxanthin preservation. Our electrochemical results were in agreement with data published by Sowmya et al.[44]. The astaxanthin specific orientation and position at the membrane level ensures a better effect both by π electron cloud and hydroxyl groups with respect to lutein that is effective mainly due to π electron cloud according to its orientation into the membrane.

$PC/Fe_3O_4$ sensors response on assessing the efficacy of standard synthetic astaxanthin was checked even in flow experiments (Fig. 8), these experiments proving $PC/Fe_3O_4$ sensor feasibility for potential in line measurements. The use of two flow lines ensures the possibility to obtain directly the relative percent of lipoperoxide formation since the signal corresponding to peroxidation $i_{FR}^{PCOO\bullet}$ is measured to one detector whereas the signal corresponding to antioxidant preservative effect, $i_{FR+Aox}^{PCOO\bullet}$ is measured simultaneously at the second detector (see flow system scheme in supplementary information, Fig. 4S).

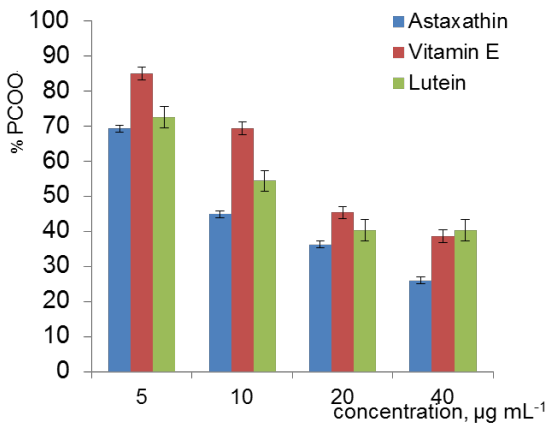


Figure 7. Variation of inhibition of PC peroxidation with antioxidant concentration

The results obtained by using the developed sensor were compared to those obtained for the same standard compounds when ORAC assay was used. The Trolox Equivalent (TE) per microgram compound being 4.88 µmol$L^{-1}$ TE/µg astaxanthin;

3.79 μmolL$^{-1}$ TE/μg vitamin E and 4.71 μmolL$^{-1}$ TE/μg lutein. ORAC assay led to the same trend of antioxidant efficacy as results provided by our developed model.

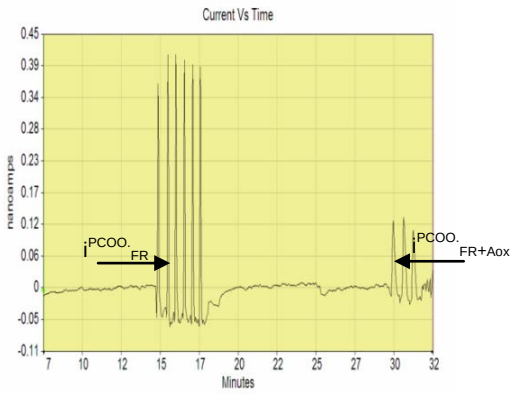


Figure 8. Chronoamperograms of PCOO peroxides signal in the absence and in the presence of astaxanthin registered at +0.385 V vs screen printed reference electrode, in flow

**Application of PC/$Fe_3O_4$ sensors in assessing astaxanthin antioxidant efficacy during accumulation in *H. pluvialis***

The developed sensors were applied to flow measurements to test the efficacy of astaxanthin during its accumulation in *H. pluvialis* at different growth stages. The astaxanthin was extracted after algal cell disruption using the protocol given in section 2.5 and the content of extracted astaxanthin determined by using UV-Vis spectrophotometry. The amount of astaxanthin so determined was used to calculate the volume of the extract injected in the measuring system in order to ensure the equivalent astaxanthin amount as used in the standard solution, namely 4.10 × 10$^{-9}$ mol L$^{-1}$. Measurements were performed after 20 minutes of incubation of free radical with PC/$Fe_3O_4$ oxidizable substrate, in astaxanthin presence. The obtained results are given in table 2, and considering the SD values, reveal that the electrochemical measurements are accurate. However, it could be emphasised that at least in the first phase of *H. pluvialis* growth (green-olive), the obtained values could be due to the presence of other carotenoids acting sinergistically.

**Table 2**. Electrochemical evaluation of astaxanthin efficacy against PCOOH formation, flow rate 2.5 mL min$^{-1}$, astaxanthin equivalent concentration 4.10×10$^{-9}$ mol L$^{-1}$

| Sample | % of generated PCOO radicals (± SD) | EAC (± SD) equivalent synthetic astaxanthin/mg dry weight |
|---|---|---|
| Astaxanthin std | 70.8 (± 0.08) | 1.00(±0.05) |
| Green stage | 81.4 (± 0.37) | 0.35 (±0.07) |
| Olive stage | 80.4 (± 0.10) | 0.88 (±0.02) |
| Brown stage | 72.7 (± 0.39) | 0.94(±0.13) |
| Red stage | 43.1 (± 0.05) | 1.65 (±0.05) |

SD- standard deviation calculated for 5 replicates

Accordingly, it should be emphasized that the obtained results are giving an overall estimation of the total antioxidant efficiency against lipoperoxidation, the method being not able to discriminate between the components. The observed antioxidant activity is fairly correlated to overall carotenoids accumulation during growth. In light stress (as it was the case of our samples provided by Algatech, Kibutz Keturra) the astaxanthin amount is increasing whereas diminishing the amounts of chlorophylls and astaxanthin precursors, the carotenoid fraction in green stage being quite exclusively composed by lutein and β-carotene while in red stages (cysts) the major carotenoid is astaxanthin. Moreover, it should be mentioned that the developed model based on oxidation of PC/$Fe_3O_4$ composite provide results regarding astaxanthin antioxidant efficacy comparable with those previously reported by Capelli et al.[51].

To properly discuss on the antioxidant efficiency of metabolites of plant origin and deliver a correct estimation of their effect, the equivalent antioxidant capacity (EAC) was calculated. The value was expressed per mg dry weight of algal mass used to obtain the same inhibition of PCOOH formation induced by 1 mg synthesized astaxanthin. Despite the fact that synthetic astaxanthin was less efficient than the astaxanthin extracted from *H. pluvialis*, the synthetic compound was used to calculate the equivalence since is less affected by lot-to-lot variability.

## Conclusions

An electrochemical sensor based on phosphatidylcholine (PC) immobilization on magnetic nanoparticles mimicking membrane lipid layers was developed and optimised in order to ensure the suitable experimental conditions in terms of carotenoids distribution in membrane (position and orientation). The obtained sensor was applied for the determination of the antioxidant efficacy of astaxanthin and proved to be useful even for other lipophilic antioxidants (vitamin E class). The PC/$Fe_3O_4$ based sensor proved to have high sensitivity equally in assessing the reactive oxygen species, ROO$^{\cdot}$ (LoD = 9.1 × 10$^{-10}$ mol L$^{-1}$) and *in situ* generated PCOO$^{\cdot}$. The sensor provided reliable information both for batch and flow measurements. The designed flow system demonstrated its applicability for *in line* control of astaxanthin accumulation subsequent algae encystment, one of the main advantages of constructed device being its capability to supply renewable surface in flow measurements thus avoiding false responses due to oxidizable substrate damaging. It was proved that storage stability of obtained PC/$Fe_3O_4$ composite is higher than 45 days.

The developed electrochemical sensor was further applied to assess the astaxanthin properties during accumulation in *H. pluvialis*, the registered responses being correlated with the expected content of carotenoids in various cysts stages. Moreover, considering the reported distribution of lutein and β-carotene at membrane level, and based on registered sensor response variability between green stage and red stage, it is obvious that the developed membrane model using immobilized PC is feasible and supply information with a better match between *in vitro* and *in vivo* measurements. It was proved that natural astaxanthin is a more effective antioxidant than synthetic astaxanthin, and that astaxanthin is more efficient than vitamin E. Our results are comparable with those reported in literature[49].

## Acknowledgements

The authors acknowledge FP7 Sensbiosyn project 232522/2009 for financial support and COST TD 1102 action for providing the opportunity of improving knowledge by fruitful debates.



 

**References**


1 G. Marrazzo, I. Barbagallo, F. Galvano, M. Malaguarnera, D. Gazzolo, A. Frigiola, N.D'Orazio and G. Li Volti, 2014, *Crit. Rev. Food Sci. Nutr.*, **54**, 1599.

2 RG Fassett and JS. Coombes, 2011, *Mar Drugs.*, **9**, 447.

3 J. Falk and S. Munné-Bosch, 2010, *J. Exp. Bot*. **61**, 1549.

4 T Lavecchia, G Rea, A Antonacci, MT Giardi, 2013, *Crit. Rev. Food Sci. Nutr*. **53**, 198.

*5* G Goswami, S Chaudhuri and D Dutta, 2010, *J Microbiol Biotechnol*, **26**, 1925.

*6* I. Po-Fung and C. Feng, 2005, *Process Biochem., **40**, 733.*

7 N. Sun, **Y.** Wanga,, Y.-T. Li, J.-*C. Huang and F. **Ch**en, 2008, Proce**ss** Biochem.* **43**, 1288.

8 M. Wan, J.Zhang, *D. Hou, J. Fan, **Y.**Li, J. Hua***ng*** and J. Wang, 2014, *Bioresour Technol*., **167**, 276.

9 W. Zhang, J. Wang, J.Wang and T. Liu, 2014, *Bioresour Technol.*, **158**, 329.

10 P. Pérez-López, S. González-García, C. Jeffryes, S. N. Agathos, E. McHugh, D. Walsh, P. Murray, S. Moane, G. Feijoo and M. T. Moreira, 2014, *J Clean Prod* **64**, 332.

11 L.B. Brentner, M.J. Eckelman and J.B Zimmerman, 2011, *Environ. Sci. Technol.* **45**, 7060.

12 R.T. Lorenz and G.R. Cysewski, 2000, *Trends Biotechnol.* **18**, 160.

13 P.Z. Margalith, 1999, *Appl. Microbiol. Biotechnol.* **51**, 431.

14 C. Hagen, S Siegmun and W. Braune, 2002, *Eur J Phycol*, **37**, 217.

15 R. Sarada, S., Bhattacharya and G.A., Ravishankar, 2002, *World J. Microbiol. Biotechnol*. **18**, 517.

16 J. Steinbrenner and H. Linden, 2003, *Plant Mol. Biol.* **52**, 343.

17 S. Boussiba, W. Bing, A. Zarka, J. P. Yuan and F. Chen, 1999, *Biotechnol Lett*, **21**, 601.

18 Y.M.A. Naguib, 2000, *J Agr Food Chem*, **48**, 1150.

19 A.Vershinin, 1999, *Biofactors*, **10**, 99.

20 G. Britton, S. Liaaen-Jensen and H. Pfander, Carotenoids Hand Book; Birkhäuser: Basel, Switzerland, 2004.

21 A. Mortensen, L.H. Skibsted, J. Sampson, C. Rice-Evans and S. A. Everett, 1997, *FEBS Lett*, **418**, 91.

22 I. Higuera-Ciapara, L. Felix-Valenzuela and F.M. Goycoolea, 2006, *Crit. Rev. Food Sci. Nutr*. **46**, 185.

23 R.R. Ambati, S.M. Phang, S. Ravi and RG Aswathanarayana, 2014, *Mar. Drugs* **12**, 128.

24 Guerin M, Huntley ME, Olaizola M. 2003, *Trends Biotechnol.* **21,** 210.

25 K Takahashi, T Takimoto, K Sato and Y. Akiba, 2011, *Anim Sci J*. **82**, 753

26 J.P. Yuan, J P.eng, K.Yin and J.H. Wang, 2011, *Mol. Nutr. Food Res.*, **55**, 150.

27 E.Yamashita, 2013, *Funct. Foods Health Dis.* **3**, 254.

28 SC Litescu, SAV Eremia and GL Radu, 2010, *Adv Exp Med Biol*, **698**, 241.

29 N J Miller and CA Rice-Evans., 1995, *Clin Sci*, **41**, 1789.

30 R Re, N Pellegrini, A Proteggente, A Pannala, M. Yang and CA Rice-Evans, 1999, *Free Rad Biol Med*, **26**, 1231.

31 Wayner DDM, Burton GW, Ingold KU and S. Locke, 1985, *FEBS Lett*, **187**, 33.

32 JM DeLong, RK Prange, DM Hodges, CF Forney, MC Bishop and M Quilliam, 2002, *J. Agric. Food Chem.*, **50**, 248.

33 B Ou, D Huang, M Hampsch-Woodill, JA Flanagan and EK Deemer 2002, *J Agric Food Chem*, **50**, 3122.

34 G H Cao, HM Alessio, and RG Cutle,r 1993, *Free Radical Biol Med*, **14**, 303.

35 C Sanchez-Moreno, 2002, *Food Sci Technol Int*, **8**, 121.

36 W. Brand-Williams, M.E. Cuvelier and C. Berset, 1995, *LWT - Food Science and Technology* **28** , 25.

37 W Bors, C Michel, M Saran and E. Lengfelder, 1978, *Biochim Biophys Acta*, **540**, 162.

38 A. A. Woodall, G. Britton, and M. J. Jackson, 1997 *Biochim Biophys Acta*, **1336**, 575.

39 T. Iyama, A. Takasuga, and M. Azuma, 1996, *Int J Vitam Nutr Res*, **66**, 301.

40 A Cantrell, D. J. McGarvey, T. G. Truscott, F Rancon and F. Beohm, 2003, *Arch Biochem Biophys* **412**, 47.

41 A. Kosteka-Gugala, D.Latowski and K. Strzalka, 2003, *Biochim Biophys Acta*, **1609**, 193.

42 Y.Matsushita, R. Suzuki, E. Nara, A. Yokoyama, and K. Miyashita, 2000, *Fisheries Sci*, **66**, 980.

43 K.Fukuzawa, Y. Inokami, A. Tokumura, J. Terrao and A. Suzuki, 1998, *Biofactors*, **7**, 31.

44 R. Sowmya and N.M. Sachindra, 2012, *Food Chem*. 134, 308.

45 M. F.Barroso, N. de-los-Santos-Álvarez, C. Delerue-Matos and M.B.P.P. Oliveira, 2011, *Biosens Bioelectron* **30**, 1–12.

46 S. C. Litescu, N. Cioffi, L. Sabbatini and G. L. Radu, 2002, *Electroanal*, **14**, 858.

47 S. C. Litescu, SAV Eremia, M Diaconu, A Tache and GL Radu, Environmental Biosensors chapter ed. Vernon Somerset, InTech, pp 95-116 , 2011.

48 M. Valko, D. Leibfritz, J. Moncol, M. T.D. Cronin, M.Mazur and J.Telser, 2007, *Int J Biochem Cell B*, **39**, 44.

49 I. Dalle-Donne, R.Rossi, R.Colombo, D.Giustarini and A. Milzani 2006, *Clin. Chem.*, **52**, 601.

50 Niki E. 1990, *Methods Enzymol.*, **186**, 100.

51 B. Capelli, D. Bagchi and G.R. Cysewski, 2013, *Nutrafoods* **12**, 145.